Experimental Investigation of Ginger Drying Using Hybrid Solar Dryer

Suherman Suherman[1*], Evan Eduard Susanto[1], Anindita Dyah Ayu[1], and Safina Dea[1]

[1] Department of Chemical Engineering, Faculty of Engineering, Diponegoro University, Jalan Prof. Soedarto, Tembalang, Semarang, Central Java, Indonesia 50275
[*] Corresponding author. E-mail: suherman.mz@che.undip.ac.id

Received: Dec. 13, 2020; Accepted: Feb. 23, 2021

Ginger is widely used as a traditional medicine for several diseases and has gained more attention due to how healthy and safe it is. Freshly harvested gingers have high moisture content and may cause product deterioration if treated incorrectly. Most ginger farmers still implement the traditional drying method, which requires a long drying time and relies heavily on the weather. In this paper, hybrid solar drying method for ginger is introduced. The performance of hybrid solar dryer, thin-layer modeling, and the quality of dried ginger were investigated. Experimental results show that in four hours of drying, only drying at 60 °C can satisfy the maximum moisture content limit of ginger, which is 12 % wet basis. The decreasing value of drying rate over time indicates that drying of ginger mostly takes place in the falling rate period. Page model is found to be the best thin-layer model to describe the behavior of ginger drying. The values of effective diffusivity are in agreement with the generally accepted value. Although the dried gingers have a good quality according to the standards, the efficiency of hybrid solar dryer is lower compared to other drying methods. Therefore, it can be concluded that hybrid solar drying is applicable for ginger due to fast drying process and acceptable quality of dried ginger, although further improvements are required.

Keywords: Ginger, Hybrid solar dryer, Thin-layer modeling, Dryer efficiency, Quality analysis

http://dx.doi.org/10.6180/jase.202108_24(4).0011

1. Introduction

Ginger (Zingiber officinale) is one of the oldest spice plants originated from South East Asia that has high potential to be cultivated for various purposes [1]. The ginger family is a tropical group, especially abundant in Indo-Malaysian region, consisting of more than 1200 plant species in 53 genera [2]. Unlike other Zingiber species, ginger has distinct anatomical features such as the absence of periderm, short-lived functional cambium, and occurrence of xylem vessels with scalariform thickening in the rhizome [3]. It is widely used around the world as a flavoring or fragrance in foods, but also in traditional oriental medicine since ancestral times. Ginger has been an integral part of the various traditional medicine for treating several diseases such as headaches, colds, muscle pains, toothache, nervous diseases, and asthma [4]. Recently, medicinal herbs such as ginger are gaining importance in mainstream healthcare as more people begin to seek for safer remedies [5].

In 2017, Indonesia ranks fifth in ginger production around the world, behind India, China, Nigeria, and Nepal [6]. In 2018, according to the Statistics Indonesia, Indonesia had exported 3,203 tonnes of gingers with Free On Board (FOB) value of 3.65 million dollars. However, from 2017 to 2018, the harvested area of ginger in Indonesia saw a 3.32 % decrease, as well as declining production, from 216,587 tonnes to 207,412 tonnes [7]. One of the problems encountered during the whole ginger production process is the postharvest processing. Most ginger rhizomes are sold commercially as fresh vegetable without processing, despite having a high moisture content during harvest (up to 82 % wet basis) [8]. This high moisture content will promote microbial growth and undesirable biochemical changes, while also increasing the cost of packaging, storage, and transportation. Therefore, proper drying process is a major concern [9, 10]. According to Indonesian National Standard [11], the maximum moisture content, ash content and foreign objects allowed in dry ginger product are 12 % wet basis, 8 %, and 2 % respectively, while the fat content should be at least 1,5 %. The unique odor and taste of ginger must be retained in the dry ginger product while molds and insects are not allowed to be present.

To this date, most ginger farmers in Indonesia still implement the conventional method to dry the ginger, by drying it directly under the sun. However, this method requires long drying time, has a high risk of contamination from dust or insects due to the exposure to the environment during drying, and unable to operate during bad weather or during rainy season [12, 13]. These disadvantages will degrade the food quality and ultimately results in a negative trade potential and economical worth. On the other hand, while using mechanical energy-driven dryers will greatly reduce drying time and prevent product deterioration, they are not economical because of the high cost and generally not favorable by traditional farmers who mostly live on rural areas [14].

Due to the complexity of the measurements of some variables during drying process, mathematical models can be used to simulate the distribution of temperature, moisture, and velocity among other variables [15]. Thin-layer drying is the procedure of drying one single layer of particles or slices of a product. The thin-layer equations predict the temporal evolution of the moisture contents of the samples, based on empirical models of the drying process, such as Newton, Page, and Modified Page models, among others. Thin-layer modeling has been widely used to study the drying kinetics or to obtain the effective diffusivity coefficient of various agricultural products [16].

Based on several problems that are still present on conventional drying, solar dryer is a favorable solution. Although there are many types of solar dryers available, generally solar dryer consists of a closed-shaped housing which acts as a "drying chamber", air ducts at the side, and a transparent cover to absorb solar radiation. This will protect the product from contamination as well as making drying process much easier to control. Solar dryer has been widely used for drying various commodities [17]. The main advantage of solar dryer over another dryer types is its utilization of solar energy, which is a renewable energy that is free, limitless, and economically viable for local farmers [18] Several researchers have studied the applications of solar dryer for ginger drying [10, 12, 14]. All studies reported that their solar dryers were able to reduce ginger's moisture content to the safe level, although drying times vary from 10 to 33 hours.

However, despite the advantages solar dryer may give, it is still reliant to solar radiation, therefore it cannot be used during the rainy season. To solve this problem, another heat source can be integrated to the existing solar dryer. This will enable the dryer to operate even without the presence of solar radiation. These dryers are called "hybrid solar dryers" [19]. To the best of authors' knowledge, there are no study or literature that discuss the application of hybrid solar dryer for ginger drying. Therefore, the aim of this paper is to investigate the application of hybrid solar dryer for ginger drying. In this study, Liquefied Petroleum Gas (LPG) is used as an auxiliary heater to support the solar dryer. Several analysis such as moisture content curve, drying rate curve, dryer efficiency, and product quality were analyzed. Thin-layer modeling was also performed to determine the best model that can accurately describe the drying behavior of ginger using hybrid solar dryer.

2. Theory and formula

After the drying processes have been finished, the experimental data can be used to perform several analyses, such as moisture content, drying rate, dryer efficiency and thin-layer modelling.

2.1. Determination of Moisture Content

Using the measurement data of ginger mass obtained from the experiment, the ginger's moisture content (M) in wet basis at specific time can be calculated using Eq.1 [20]. m_i is the mass of wet ginger (g) while m_d is the mass of dry ginger (g).

$$M = \frac{m_i - m_d}{m_i} \times 100\% \quad (1)$$

2.2. Determination of Drying Rate

The drying rate (R_d, g/minutes) was determined by dividing the difference of ginger's mass (g) at two consecutive measurement ($m_{t+\Delta t} - m_t$) and the time interval (t, minutes), as shown in Eq.2 [20].

$$R_d = \frac{m_{t+\Delta t} - m_t}{t} \times 100\% \quad (2)$$

2.3. Determination of Dryer Efficiency

The ginger mass and solar radiation data measured from the experiment can be further processed to obtain dryer efficiency, using Eq.3 [21].

$$\eta_d = \frac{m_w . h_{fg}}{IAt + E + m_{fuel} . C_v} \times 100\% \quad (3)$$

Where η_d is dryer efficiency (%), m_w is the total mass of evaporated water (kg), h_{fg} is water's latent heat of vaporization, I is the solar radiation (W/m^2), A is the area of solar collector (m^2), t is the drying time (s), E is the energy consumption by the blower (kJ), m_{fuel} is the mass of fuel used (kg), and C_v is the heating value of LPG (kJ/kg).

2.4. Thin-layer Modelling

In this experiment, seven thin-layer drying models were used to determine the most suitable model that can describe the drying behavior of ginger using hybrid solar dryer. The modeling was carried out using MATLAB software. Table 1 shows the drying models used. These thin layer drying models are often used on fruits and vegetables [22]. A new parameter, namely Moisture Ratio (MR) is defined using Eq.4 [23].

$$MR = \frac{M - M_e}{M_o - M_e} \times 100\% \quad (4)$$

M is the moisture content at any given time, while M_o is the initial moisture content, and M_e is the equilibrium moisture content. However, in this experiment, the relative humidity values varied continuously during drying and the values of M_e are relatively small compared to M or M_o [23, 24]. Therefore, Eq.4 can be simplified into Eq.5.

$$MR = \frac{M}{M} \times 100\% \quad (5)$$

Three parameters were used to evaluate the accuracy of the drying models, namely correlation coefficient (R^2), Root Mean Square Error ($RMSE$), and reduced chi-square (χ^2) The model with the highest value of R^2 and lowest value of both $RMSE$ and χ^2 will be chosen as the most suitable model [25]. The value of R^2, $RMSE$, and χ^2 can be determined using Eq. (6-8) [14, 26]. MR_{exp} is moisture ratio from experimental data, MR_{pre} is predicted moisture ratio using thin-layer drying models, while straight lines above MR_{exp} or MR_{pre} indicate average value. N is the number of observations and n is the number of constants in drying model.

$$RMSE = \sqrt{\frac{1}{N}\sum_{i=1}^{N}(MR_{exp,i} - MR_{pre,i})^2} \quad (6)$$

$$R^2 = \frac{\left[\sum_{i=1}^{N}(MR_{exp,i} - \overline{MR_{exp}})(MR_{pre,i} - \overline{MR_{pre}})\right]^2}{\sum_{i=1}^{N}(MR_{exp,i} - \overline{MR_{exp}})^2 sum_{i=1}^{N}(MR_{pre,i} - \overline{MR_{pre}})^2} \quad (7)$$

$$\chi^2 = \frac{\sum_{i=1}^{N}(MR_{exp,i} - MR_{pre,i})^2}{N - n} \quad (8)$$

Ertekin and Firat [27] have stated that drying characteristics in the falling rate period can be described using Fick's diffusion equation. Assuming long drying time, uniform moisture distributions, and slab geometry for ginger, the value of effective diffusivity (D_{eff}) can be determined using Eq. 9 [28].

$$MR = \frac{8}{\pi^2} exp\left[\frac{D_{eff}\pi^2}{4L^2}t\right] \quad (9)$$

Where D_{eff} is effective diffusivity (m^2/s), L is the half-thickness of ginger (m), t is drying time (s), and π is a constant. By changing Eq. 9 into logarithmic form, a new linear equation is obtained, as shown in Eq. 10. The value of D_{eff} can be obtained by plotting MR and t in a linear graph. All calculations of D_{eff} are performed using Microsoft Excel.

$$\ln MR = \ln \frac{8}{\pi^2} exp\left[\frac{D_{eff}\pi^2}{4L^2}t\right] \quad (10)$$

2.5. Quality Analysis

To determine the quality of dried ginger, four quality parameters were analyzed, namely aroma, fat content, ash content, and the presence of molds and insects in the ginger sample. All quality analyses were performed at the Integrated Laboratory of Diponegoro University. Ash content was analyzed using electrical furnace at 550 °C, while fat content was determined by solvent extraction method [29].

3. Experimental setup

The hybrid solar dryer can be divided into two parts, namely drying chamber and blower and burner unit, as shown in Fig. 1. The drying chamber is box-shaped, with dimensions of 90 cm in length, 90 cm in width, and 120 cm in height. The outer frame of the drying chamber was covered by aluminium with 1 mm thickness, which gives the dryer good heat conductivity, as well as for protection due to its good strength. The inside wall of the drying chamber was covered by stainless steel with 1.2 mm thickness for strengthening purposes and further increases the heat conductivity of the dryer as a whole. Glass wool was added to the inside wall as an insulating material due to its high thermal insulating properties. An acrylic panel with 90 cm in both length and width and 0.5 cm thick was installed at the top of the dryer, which acted as solar radiation absorber and placed diagonally for better absorbance of solar radiation. Four wheels were installed at the bottom edge of the dryer for transporting purposes and to adjust the dryer's position for maximum solar radiation absorption.

Fig. 2a shows the inside view of the drying chamber. Three drying trays, each with 80 cm in length and 80 cm in width were placed inside the drying chamber. The trays were made from perforated wire so drying air may pass through from the bottom to the top. The humid drying air would exit through a circular duct installed at the top of the dryer. The edges of each tray were covered with aluminum for heat conducting purposes as well as to ease the placement of trays to the tray holders which were installed at the left and right sides of the drying walls. At each drying tray, the top, and the bottom wall of the drying chamber, temperature and relative humidity indicators

Table 1. Thin-layer drying models [22].

No	Thin-layer Models	Formula
1	Newton	MR = exp (-kt)
2	Page	MR = exp (-kt^n)
3	Modified Page	MR = exp [-(kt)^n]
4	Midilli et al.	MR = a exp (-kt) + bt
5	Modified Midilli et al.	MR = a exp (-kt) + b
6	Approximation of Diffusion	MR = a exp(-kt) + (1-a) exp (-kbt)
7	Demir et al.	MR = a exp(-kt)^n + b

Fig. 1. Complete view of hybrid solar dryer system.

were installed. These data can be read in the LCD placed inside the control panel at the left side of the dryer. At the right side of the drying chamber, a pipe was installed to connect the air pipe containing drying air from the blower unit. Meanwhile, Fig. 2b shows the blower and burner unit. In this unit, Liquefied Petroleum Gas (LPG) will heat the drying air through the burner unit. At the side end of the unit, a blower unit blew the air, passing through the burner section (in which the drying air would heat up), and flew to the drying chamber through air pipes that connected the burner unit and the drying chamber. A control panel was installed at the burner unit to monitor the drying temperature. The on/off switch for the burner unit was located inside this control panel.

The main material used in this experiment was fresh ginger rhizomes, obtained from ginger farmers in Ungaran, Semarang, Indonesia. The harvesting age of the fresh rhizomes was nine months. The supporting tools required were stopwatch, digital mass balance, plastic sheet temperature and relative humidity meter (@Krisbow S000052505), and SM206 Solar power meter. This experiment was performed at the Laboratory of Department of Chemical Engineering, Diponegoro University. During hybrid solar

(a) Inside view of the drying chamber

(b) Blower and burner unit

drying, the independent variables used were tray locations (tray 1 is in the bottom while tray 3 is located at the top) and drying temperatures (40, 50, and 60 °C). The fixed variables were drying time (4 hours, from 10:00 A.M. to 02:00 P.M), initial moisture content of ginger rhizomes (82.6 % wet basis), and the weight of gingers on each tray, which was 100 grams. Initial moisture content of ginger rhizomes was obtained using oven method [29].

Before drying process began, fresh ginger rhizomes were washed, then the outer thin layer of the rhizomes were peeled. After that, the rhizomes were cut horizontally with 5 mm thickness. Next, 300 grams of ginger rhizomes were placed equally on three drying trays to undergo drying process. However, before the drying process began, the dryer must be prepared first. Firstly, the blower is connected to the bottom part of the drying chamber using air pipes. Next, the LCD was turned on using switch inside the control panel. After that, the LPG heater can be turned on to set the desired drying temperature, and let the dryer run without any load for awhile. This served as a means to calibrate the dryer. At the first day, drying process was done with dryer temperature of 40 °C, second day with drying temperature of 50 °C, and the third day with drying temperature of 60 °C. The temperature and relative humidity data at the dryer inlet, outlet, and at the each tray were displayed on the LCD. The solar intensity near the collector was measured using solar power meter. Every 30 minutes, the ginger rhizomes were taken out and weighed using digital mass balance to determine the weight reduction.

4. Results and Discussions

4.1. Temperature, relative humidity, and solar intensity profiles

The measurement data of temperatures, relative humidity, and solar radiation were put into a graph to understand its relation with drying time. Fig. 3 shows the profiles of temperature, relative humidity, and solar intensity at drying with the temperature of 60 °C, which was performed at the third day of experiment. It can be seen from Fig. 3 that the ambient temperature varied from 29 to 33 °C while the solar intensity varied between 845.54 to 1510.72 W/m^2, with the average of 1178.13 W/m^2. It was observed that the outlet temperature was lower than drying chamber temperature. This indicates that the drying air exiting the dryer carries higher moisture compared to when it first entered the dryer, which proves that drying process does occur [30]. The temperature of the drying chamber remained relatively stable (between 60-65 °C) throughout the drying process due to the addition of LPG heater. The dryer is designed to trap the heat inside it, which can help maintaining relatively stable temperature inside the dryer. This may explain why the highest dryer temperature was recorded at 12:30, even though the solar radiation at that time was not the highest. However, the dryer temperature began to decrease at 12:30 onwards due to decreasing solar radiation. Contrary to the temperature, relative humidity profiles are shown to be increasing as drying continues. These findings about the temperature and relative humidity profiles were also found on similar hybrid solar dryer researches [20, 21, 31].

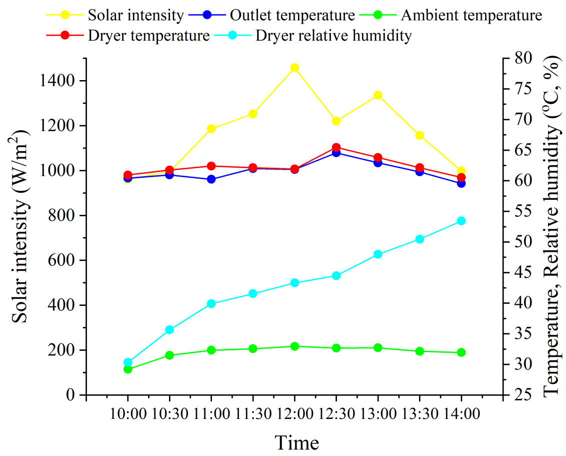

Fig. 3. The profiles of temperature, relative humidity, and solar intensity during hybrid solar drying at 60 °C.

4.2. Moisture content analysis

Fig. 4 shows the moisture content curve at different temperature and at the top tray, while Fig. 5 shows the moisture content curve at different trays during drying at 60 °C. As seen in Fig. 4, drying with higher temperature resulted in faster moisture reduction. High drying air temperature means the drying air is less humid, therefore it is able to evaporate and take more moisture from ginger [19, 32]. The final moisture content of ginger dried at the temperature of 40, 50, and 60 °C was 29.12 %, 13.39 %, and 9.61 %, respectively, all in wet basis. Comparing these final moisture content results to the safe limit stated by Indonesian National Standard (maximum 12 % w.b.), only drying at 60 °C is satisfactory. However, considering the time required to dry the ginger into safe moisture content, hybrid solar dryer used in this experiment is much faster than other types of dryers for ginger drying studied by several researchers [5, 10, 14].

The final moisture content of ginger dried at the top, middle, and bottom tray during drying at 60 °C was 9.61 %, 10.45 %, and 11.72 %. From Fig. 5, it can be seen that the fastest moisture reduction ocurred at the top tray. The solar dryer used in this experiment was a direct type, combined

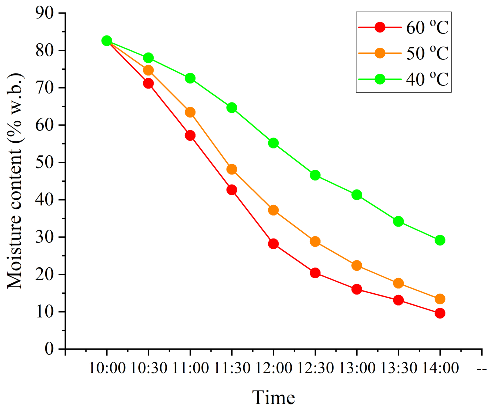

Fig. 4. Moisture content curve at different temperatures during drying at the top tray.

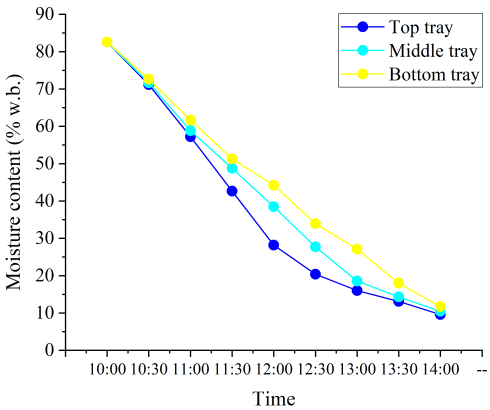

Fig. 5. Moisture content curve at different trays during drying at 60 °C.

with indirect heating by LPG. The heat from LPG entered the bottom tray first while heat from the solar radiation entered from the top. This interaction caused the top tray to gain more heat compared to the middle tray or bottom tray. The aluminum covering enabled the dryer to store high amount of heat obtained from solar radiation. This explains why the top tray is the hottest despite the drying air flows from the bottom tray first [33–35].

4.3. Drying rate analysis

Fig. 6 shows the drying rate curve of ginger at different temperatures at the top tray, while Fig. 7 shows the drying rate curve of ginger at different trays during drying at 60 °C. It can be seen from Fig. 6 that using higher drying temperature would increase the drying rate, while from Fig. 7, the tray locations did not affect the drying rate, although drying at the top tray yielded slightly higher value of drying rate. This phenomenon was also found on other solar drying researches that utilized trays in their drying chambers [14, 35]. The average drying rate during drying at the top tray at 40, 50, and 60 °C was 0.31, 0.33, and 0.34 g/minutes respectively. During drying at high temperature, the partial vapor pressure difference between drying air and ginger became higher, which increased the evaporation rate [36].

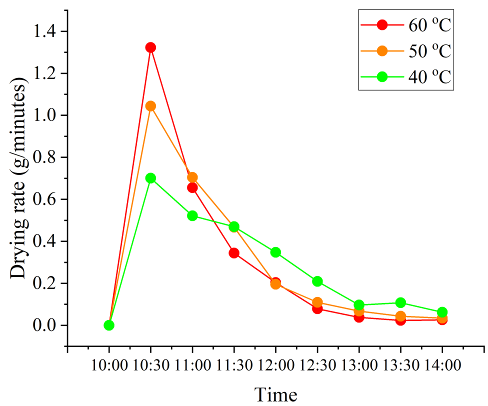

Fig. 6. Drying rate curve of ginger at different temperatures during drying at the top tray.

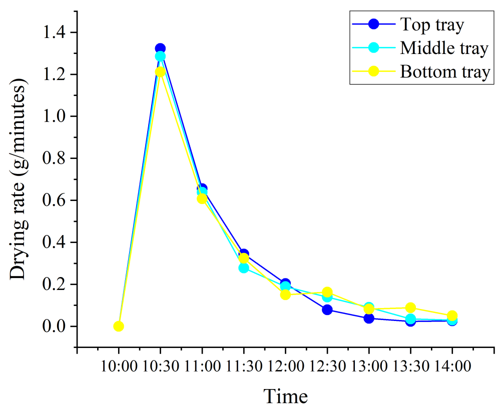

Fig. 7. Drying rate curve of ginger at different trays during drying at 60 °C.

From both Figs. 6 and 7, it can be seen that the value of drying rate was intitially high, then gradually decreased as drying process continues. This indicated that drying of ginger primarily took place at the falling rate period, proved by the decreasing value of drying rate over time [37]. During initial hours of drying, there was still high moisture transport from the ginger's surface to the ambient. At the later part of the drying, the moisture from ginger's inner core would migrate to the surface. At this point, the moisture transport from ginger's surface to the ambient became lower, hence the drying rate was decreasing in the last stage of the drying process [38].

4.4. Dryer efficiency analysis

Fig. 8 shows the curve of dryer efficiency during drying at different temperatures. The range of dryer efficiency during drying at 40, 50, and 60 °C was 3.76 - 18.7 %, 1.04 – 33.16 %, and 1.09 – 44.62 %, respectively. The average dryer efficiency at 40, 50, and 60 °C was 9.64 %, 10.31 %, and 10.86 % respectively. It can be seen that using higher drying temperature would increase the dryer efficiency. This happens because higher drying temperature used will generate more heat, which will increase the moisture uptake by drying air and speeds up the drying process. This will increase the dryer efficiency [39, 40]. However, the values of dryer efficiency found in this experiment are lower compared to other similar studies. Murali et al. (2020) reported that energy efficiency of solar LPG hybrid dryer applied for shrimps were varied from 24.21 to 37.09 %, with the average value of 29.93 %. Aviara et al. (2014) found that using tray dryer for cassava starch drying, dryer efficiency was increased from 16 % to 30 % when drying temperature increased from 40 °C to 60 °C. Fudholi et al. (2014) reported an average dryer efficiency value of 27.1 % during seaweed drying using solar tray dryer.

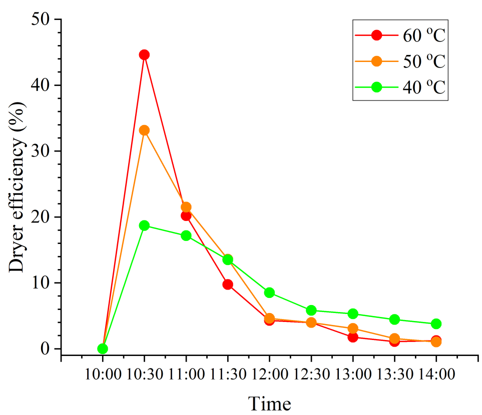

Fig. 8. Dryer efficiency curve at different drying temperatures.

The maximum dryer efficiency during drying at 40, 50, and 60 °C was 18.7 %, 33.16 %, and 44.62 % respectively. It can be seen from Fig. 8 that dryer efficiency reached maximum value at the start of the drying, then gradually decreased over time. During the initial phase of drying, the ginger's surface was saturated with free moisture, which will be evaporated first by the drying air. As drying process continues, the free moisture at the ginger's surface became fewer and the moisture at the inner structure of the ginger began to diffuse from the inner structure to the surface of ginger. This will reduce the moisture uptake of the drying air, which also reduce the value of dryer efficiency [10, 41].

4.5. Mathematical modelling

The moisture ratio data obtained from the experiment were plotted into seven thin-layer drying models to find the suitable model that can accurately describe the drying behavior of ginger using hybrid solar dryer. It should be noted that the thin-layer modeling was only performed at the top tray because it had the fastest moisture reduction and yielded the best result compared to the middle and bottom tray. Table 2 shows the thin-layer modeling results for each model at different temperature, including all of the empirical constants of the thin-layer models (k, n, a, and b) as well as the values of R^2, $RMSE$, and χ^2.

A thin-layer model is said to be suitable to the experimental data if it has high R^2 value (close to one) as well as low $RMSE$ and χ^2 value. By taking average value of all the parameters of every thin-layer model at different temperatures, Page model is the most suitable model. The average R^2, $RMSE$, and χ^2 value of Page model is 0.9966, 0.0171, and 0.0004 respectively. Modified Page model and Midilli et al. model. also fits well since the parameter values only differ slightly. Similar research about thin-layer drying of ginger using solar dryer also reported that Page model showed the best fit to experimental data [14]. Page model has also been adopted by American Standard as a standard model for thin-layer drying of most agricultural and biological products [22]. Eqs. (11-13) show the MR equation of ginger drying using Page model at 40, 50, and 60 °C, respectively, with t in minutes.

$$MR = \exp(-0.0006t^{1.3730}) \tag{11}$$

$$MR = \exp(-0.0009t^{1.4126}) \tag{12}$$

$$MR = \exp(-0.0027t^{1.2297}) \tag{13}$$

Fig. 9 shows the curve fitting of Page model against the experimental data at 60 °C. It can be seen that the predicted values using Page model are scattered close to the diagonal lines (representing the experimental data), indicating Page model shows a good fit with moisture ratio data of ginger during drying. Both curve fitting of Page model at 40 and 50 °C also exhibit good fit, although the curves are not presented here. Similar results can also be found on

Table 2. Thin-layer drying modelling results.

Models	T (°C)	k	n	A	b	R^2	RMSE	χ^2
Newton	40	0.0036				0.9785	0.0480	0.0026
	50	0.0064				0.9856	0.0500	0.0028
	60	0.0081				0.9860	0.0471	0.0025
Page	40	0.0006	1.3730			0.9979	0.0118	0.0002
	50	0.0009	1.4126			0.9969	0.0168	0.0004
	60	0.0027	1.2297			0.9950	0.0228	0.0007
Modified Page	40	0.0039	1.1578			0.9914	0.0309	0.0012
	50	0.0067	1.2652			0.9971	0.0185	0.0004
	60	0.0081	1.2192			0.9949	0.0234	0.0007
Midilli et al.	40	0.0016		1.0020	-0.0013	0.9926	0.0265	0.0011
	50	0.0051		1.0020	-0.0006	0.9904	0.0347	0.0018
	60	0.0074		1.0020	-0.0002	0.9878	0.0403	0.0024
Modified Midilli et al.	40	0.0049		0.8228	0.8660	0.9655	0.0546	0.0045
	50	0.0077		0.904	0.0941	0.9781	0.0604	0.0055
	60	0.0102		0.9272	0.0934	0.9748	0.0579	0.0050
Approximation of Diffusion	40	0.0016		1.9297	0.0134	0.9903	0.0331	0.0016
	50	0.0030		1.8645	0.1627	0.9896	0.0321	0.0015
	60	0.0061		1.6476	0.6333	0.9884	0.0405	0.0025
Demir et al.	40	0.0122	0.4975	0.4942	0.5111	0.9748	0.0536	0.0052
	50	0.0203	0.5131	0.5620	0.4688	0.9905	0.0286	0.0015
	60	0.0195	0.5387	0.6300	0.3897	0.9872	0.0349	0.0022

thin layer-drying of turmeric [24], cashew kernels [42], and apricot kernels [43].

Table 3. Effective diffusivity of ginger.

No	Temperature (°C)	Effective diffusivity (m^2/s)
1	40	2,57 x 10^{-10}
2	50	4,65 x 10^{-10}
3	60	5,62 x 10^{-10}

It has been widely accepted that during drying at the falling rate period, Fick's second law can be applied as drying is mainly controlled by diffusion [43]. Table 3 shows the effective diffusivity (D_{eff}) values of ginger dried at different temperatures. It can be seen that the values of effective diffusivity increase when higher temperature is used. An increase in temperature will increase the vapor pressure inside the ginger. This will cause the rapid movement of water molecules inside the ginger since the water molecules are loosely bound to the inner structure of the ginger [44]. The D_{eff} values found in this experiment were in the range of 10^{-11} to 10^{-9} m^2/s, which is a general range of effective diffusivity value for most agricultural and food products [45]. Deshmukh et al. [14] reported that the effective diffusivity of ginger using solar drying is 1.789 x 10^{-9} m^2/s. Other researches about thin-layer modeling also reported similar values of D_{eff}, from 3.23 x 10^{-10} to

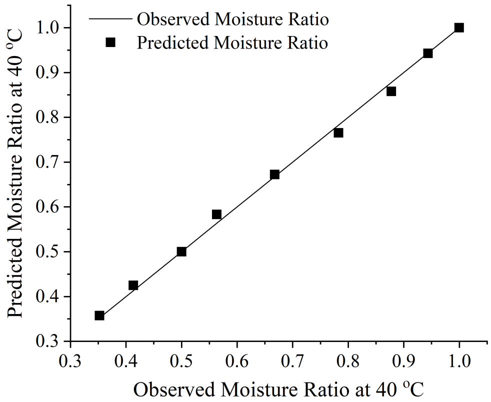

Fig. 9. Curve fitting of Page model and experimental data at 60 °C.

7.82 x 10^{-10} m^2/s for quince slices [28], from 1.39 x 10^{-8} to 3.5 x 10^{-8} m^2/s for apricot kernels [43], and from 7.2 x 10^{-9} to 1.91 x 10^{-8} m^2/s for sorghum stalk [46].

4.6. Quality of dried ginger

Four quality parameters of dried ginger that were tested in this experiment consisted of aroma test, fat content, ash content, and presence of molds and insects during storage Table 4 shows the value of ginger's quality parameters dried at different temperatures compared to the standard value, as governed by Indonesian National Standard.

During the quality test, there were no changes in dry ginger's aroma, also no molds and insects were present during storage of dried ginger. Both fat and ash contents of dried ginger have satisfy the range of their respective standard value. It can be seen from table 4 that fat content decreases when higher temperature is used. This happens because higher temperature will deactivate the enzymes, thus halting the production of volatile fatty compounds and reducing fat content [47]. However, drying helps conserve the bioactive compounds and unsaturated fatty acids which are more adequate for consumption [48].

5. Conclusions

An investigation and thin-layer modeling of ginger drying using hybrid solar dryer has been performed. It was found that only final moisture content of ginger dried at 60 °C gives the best result according to the Indonesian National Standard. However, the drying process only takes four hours, which is much faster than other ginger drying studies using other types of dryer. It is implied that ginger drying mostly happens at the falling rate period, indicated by decreasing value of drying rate over time. Page model is found to be the best model to describe drying behavior of ginger. The effective diffusivity values of ginger in this experiment are in the range of standard values of most agricultural products. It is shown that hybrid solar drying does not affect the aroma of ginger and no molds or insects are present during storage. The fat and ash contents of dried ginger in this experiment are in accordance to the Indonesian National Standard. It can be concluded that hybrid solar drying method introduced in this study is suitable for ginger and much faster compared to other methods of ginger drying, while still able to maintain the quality of dried ginger. However, the dryer efficiency in this experiment is lower compared to other similar studies about solar drying. Therefore, further investigation and optimization of hybrid solar dryer is required to maximize the dryer efficiency.

6. Acknowledgements

This study is funded by Director General of Scientific and Technological Development and Advancements, as a part of Indonesian Ministry of Research and Technology.

Table 4. Quality parameters of ginger dried at different temperatures.

Parameters	Parameter value			Standard Value
	40 °C	50 °C	60 °C	
Aroma	ginger	ginger	ginger	Unique, ginger-like
Fat content (%)	5.56	3.44	2.93	1.5 % min.
Ash content (%)	2.93	4.18	4.77	8% max.
Molds and insects	Not present	Not present	Not present	Not present

References

[1] Kejing An, Dandan Zhao, Zhengfu Wang, Jijun Wu, Yujuan Xu, and Gengsheng Xiao. Comparison of different drying methods on Chinese ginger (Zingiber officinale Roscoe): Changes in volatiles, chemical profile, antioxidant properties, and microstructure. *Food Chemistry*, 197:1292–1300, 2016.

[2] A. Angeline Rajathi, A. Allwyn Sundarraj, Shilu Leslie, and M. M. Pragalyaashree. Processing and medicinal uses of cardamom and ginger - A review. *Journal of Pharmaceutical Sciences and Research*, 9(11):2117–2122, 2017.

[3] Jaleel Kizhakkayil and B. Sasikumar. Diversity, characterization and utilization of ginger: A review. *Plant Genetic Resources: Characterisation and Utilisation*, 9(3):464–477, 2011.

[4] Huijuan Li, Yanan Liu, Dan Luo, Yuzhen Ma, Jie Zhang, Meixuan Li, Liang Yao, Xiue Shi, Xingrong Liu, and Kehu Yang. Ginger for health care: An overview of systematic reviews. *Complementary Therapies in Medicine*, 45(March):114–123, 2019.

[5] Khanuengnit Chapchaimoh, Nattapol Poomsa-Ad, Lamul Wiset, and John Morris. Thermal characteristics of heat pump dryer for ginger drying. *Applied Thermal Engineering*, 95:491–498, 2016.

[6] FAO. Crops - Cassava, 2020.

[7] Statistics Indonesia. Statistics of Medicinal Plants Indonesia. 2018.

[8] Singhanat Phoungchandang and Supawinee Saentaweesuk. Effect of two stage, tray and heat pump assisted-dehumidified drying on drying characteristics and qualities of dried ginger. *Food and Bioproducts Processing*, 89(4):429–437, 2011.

[9] S. H. Ding, K. J. An, C. P. Zhao, Y. Li, Y. H. Guo, and Z. F. Wang. Effect of drying methods on volatiles of Chinese ginger (Zingiber officinale Roscoe). *Food and Bioproducts Processing*, 90(3):515–524, 2012.

[10] D. K. Rabha, P. Muthukumar, and C. Somayaji. Energy and exergy analyses of the solar drying processes of ghost chilli pepper and ginger. *Renewable Energy*, 105:764–773, 2017.

[11] Indonesian National Standard. *SNI 01-3393-1994 - Jahe Kering*, 1994.

[12] Elsamila Aritesty and Dyah Wulandani. Performance of the rack type-greenhouse effect solar dryer for wild ginger (curcuma xanthorizza roxb.) drying. *Energy Procedia*, 47:94–100, 2014.

[13] Jnyana R. Pati, Santosh K. Hotta, and P. Mahanta. Effect of waste heat recovery on drying characteristics of sliced ginger in a natural convection dryer. *Procedia Engineering*, 105(Icte 2014):145–152, 2015.

[14] A. Waheed Deshmukh, Mahesh N. Varma, Chang Kyoo Yoo, and Kailas L. Wasewar. Investigation of Solar Drying of Ginger (Zingiber officinale): Emprical Modelling, Drying Characteristics, and Quality Study. *Chinese Journal of Engineering*, 2014:1–7, 2014.

[15] A. M. Castro, E. Y. Mayorga, and F. L. Moreno. Mathematical modelling of convective drying of fruits: A review. *Journal of Food Engineering*, 223:152–167, 2018.

[16] L. Blanco-Cano, A. Soria-Verdugo, L. M. Garcia-Gutierrez, and U. Ruiz-Rivas. Modeling the thin-layer drying process of Granny Smith apples: Application in an indirect solar dryer. *Applied Thermal Engineering*, 108:1086–1094, 2016.

[17] Om Prakash, Vinod Laguri, Anukul Pandey, Anil Kumar, and Arbind Kumar. Review on various modelling techniques for the solar dryers. *Renewable and Sustainable Energy Reviews*, 62:396–417, 2016.

[18] Laszlo Imre. Solar Drying. In Arun S. Mujumdar, editor, *Handbook of Industrial Drying*, volume 4, chapter 13, pages 308–363. CRC Press, Florida, 4 edition, 2014.

[19] David Gudiño-Ayala and Ángel Calderón-Topete. Pineapple drying using a new solar hybrid dryer. *Energy Procedia*, 57:1642–1650, 2014.

[20] S. Murali, P. R. Amulya, P. V. Alfiya, D. S.Aniesrani Delfiya, and Manoj P. Samuel. Design and performance evaluation of solar - LPG hybrid dryer for drying of shrimps. *Renewable Energy*, 147:2417–2428, 2020.

[21] S Dhanushkodi, Vincent H Wilson, and K Sudhakar. Design and thermal performance of the solar biomass

hybrid dryer for cashew drying. *Facta universitatis-series: Mechanical Engineering*, 12(3):277–288, 2014.

[22] Daniel I. Onwude, Norhashila Hashim, Rimfiel B. Janius, Nazmi Mat Nawi, and Khalina Abdan. Modeling the Thin-Layer Drying of Fruits and Vegetables: A Review. *Comprehensive Reviews in Food Science and Food Safety*, 15(3):599–618, 2016.

[23] Olawale Usman Dairo, Adewole Ayobami Aderinlewo, Olayemi Johnson Adeosun, Ibukun Adekola Ola, and Tolulope Salaudeen. Solar drying kinetics of cass ava slices in a mixed flow dryer. *Acta Technologica Agriculturae*, 18(4):102–107, 2015.

[24] A. K. Karthikeyan and S. Murugavelh. Thin layer drying kinetics and exergy analysis of turmeric (Curcuma longa) in a mixed mode forced convection solar tunnel dryer. *Renewable Energy*, 128:305–312, 2018.

[25] Suparerk Charmongkolpradit and Ratinun Luampon. Study of Thin Layer Drying Model for Cassava Pulp. *Energy Procedia*, 138:354–359, 2017.

[26] S. Dhanushkodi, Vincent H. Wilson, and K. Sudhakar. Mathematical modeling of drying behavior of cashew in a solar biomass hybrid dryer. *Resource-Efficient Technologies*, 3(4):359–364, 2017.

[27] Can Ertekin and M. Ziya Firat. A comprehensive review of thin-layer drying models used in agricultural products. *Critical Reviews in Food Science and Nutrition*, 57(4):701–717, 2017.

[28] Dimitrios A. Tzempelikos, Alexandros P. Vouros, Achilleas V. Bardakas, Andronikos E. Filios, and Dionissios P. Margaris. Experimental study on convective drying of quince slices and evaluation of thin-layer drying models. *Engineering in Agriculture, Environment and Food*, 8(3):169–177, 2015.

[29] S. Suzanne Nielsen. *Food Analysis*. Springer, 4th editio edition, 2010.

[30] Suherman Suherman, Mohammad Djaeni, Dyah H. Wardhani, Mukhtar R. Dzaki, and Muhammad N.F. Bagas. Performance Analysis of Solar Tray Dryer for Cassava Starch. *MATEC Web of Conferences*, 156:0–3, 2018.

[31] A. Bosomtwe, J. K. Danso, E. A. Osekre, G. P. Opit, G. Mbata, P. Armstrong, F. H. Arthur, J. Campbell, N. Manu, S. G. McNeill, and J. O. Akowuah. Effectiveness of the solar biomass hybrid dryer for drying and disinfestation of maize. *Journal of Stored Products Research*, 83:66–72, 2019.

[32] Suherman Suherman and Nur Hidayati. Performance Evaluation of Pneumatic Dryer for Aren (Arenga piñata) Flour. In *The 24th Regional Symposium on Chemical Engineering (RSCE 2017)*, volume 156, page 05023, Semarang, 2018. MATEC Web of Conferences.

[33] Tadahmun A. Yassen and Hussain H. Al-Kayiem. Experimental investigation and evaluation of hybrid solar/thermal dryer combined with supplementary recovery dryer. *Solar Energy*, 134:284–293, 2016.

[34] Evangelos Tsotsas and Arun S. Mujumdar. *Modern Drying Technology, Volume 4: Energy Savings*. Wiley-VCH, Weinheim, 2011.

[35] Ehsan Baniasadi, Saeed Ranjbar, and Omid Boostanipour. Experimental investigation of the performance of a mixed-mode solar dryer with thermal energy storage. *Renewable Energy*, 112:143–150, 2017.

[36] Hamid Mortezapour, Barat Ghobadian, Saeid Minaei, and Mohammad Hadi Khoshtaghaza. Saffron drying with a heat pump-assisted hybrid photovoltaic-thermal solar dryer. *Drying Technology*, 30(6):560–566, 2012.

[37] Mohamed A. Eltawil, Mostafa M. Azam, and Abdulrahman O. Alghannam. Energy analysis of hybrid solar tunnel dryer with PV system and solar collector for drying mint (MenthaViridis). *Journal of Cleaner Production*, 181:352–364, 2018.

[38] D. V.N. Lakshmi, P. Muthukumar, Apurba Layek, and Prakash Kumar Nayak. Drying kinetics and quality analysis of black turmeric (Curcuma caesia) drying in a mixed mode forced convection solar dryer integrated with thermal energy storage. *Renewable Energy*, 120:23–34, 2018.

[39] Ndubisi A. Aviara, Lovelyn N. Onuoha, Oluwakemi E. Falola, and Joseph C. Igbeka. Energy and exergy analyses of native cassava starch drying in a tray dryer. *Energy*, 73:809–817, 2014.

[40] Alejandro Reyes, Andrea Mahn, and Francisco Vásquez. Mushrooms dehydration in a hybrid-solar dryer, using a phase change material. *Energy Conversion and Management*, 83:241–248, 2014.

[41] Ahmad Fudholi, Kamaruzzaman Sopian, Mohd Yusof Othman, and Mohd Hafidz Ruslan. Energy and exergy analyses of solar drying system of red seaweed. *Energy and Buildings*, 68(PARTA):121–129, 2014.

[42] W.B. Asiru, A.O. Raji, J.C. Igbeka, and G.N. Elemo. Mathematical Modelling of Thin Layer Dried Cashew Kernels. *Nigerian Food Journal*, 31(2):106–112, 2013.

[43] Qing-An Zhang, Yun Song, Xi Wang, Wu-Qi Zhao, and Xue-Hui Fan. Mathematical modeling of debittered apricot (Prunus armeniaca L .) kernels during thin-layer drying . *CyTA - Journal of Food*, 14(4):509–517, 2016.

[44] O. R. Alara, N. H. Abdurahman, and O. A. Olalere. Mathematical modelling and morphological properties of thin layer oven drying of Vernonia amygdalina

leaves. *Journal of the Saudi Society of Agricultural Sciences*, 18(3):309–315, 2019.

[45] Ndubisi A. Aviara and Joseph C. Igbeka. Modeling for Drying of Thin Layer of Native Cassava Starch in Tray Dryer. *Journal of Biosystems Engineering*, 41(4):342–356, 2016.

[46] Fei Shen, Lin Peng, Yanzong Zhang, Jun Wu, Xiaohong Zhang, Gang Yang, Hong Peng, Hui Qi, and Shihuai Deng. Thin-layer drying kinetics and quality changes of sweet sorghum stalk for ethanol production as affected by drying temperature. *Industrial Crops and Products*, 34(3):1588–1594, 2011.

[47] Jun Qiu, Parag Acharya, Doris M. Jacobs, Remko M. Boom, and Maarten A.I. Schutyser. A systematic analysis on tomato powder quality prepared by four conductive drying technologies. *Innovative Food Science and Emerging Technologies*, 54(October 2018):103–112, 2019.

[48] Aicha Jelled, ngela Fernandes, Lillian Barros, Hassiba Chahdoura, Lotfi Achour, Isabel C.F.R. Ferreira, and Hassen Ben Cheikh. Chemical and antioxidant parameters of dried forms of ginger rhizomes. *Industrial Crops and Products*, 77:30–35, 2015.